# MHD considerations for the DCLL inboard blanket and access ducts

Sergey Smolentsev [a,*], Clement Wong [b], Siegfried Malang [c], Mo Dagher [a], Mohamed Abdou [a]

[a] University of California, MAE, 43-133 Engineering IV, Los Angeles, CA 90095-1597, USA
[b] General Atomics, San Diego, USA
[c] Fliederweg 3, D 76351 Linkenheim-Hochstetten, Germany

## ABSTRACT

The pre-conceptual design for the US DEMO inboard dual-coolant lead–lithium breeding blanket is introduced for the first time followed by the assessment for the most important magnetohydrodynamic issues for the blanket module itself and access ducts. The considered issues include: (i) the magnetohydrodynamic pressure drop, (ii) electric insulation in poloidal flows using the silicon carbide flow channel insert, and (iii) countercurrent flows in the access ducts.

Published by Elsevier B.V.

First, we introduce the pre-conceptual design for the US DEMO inboard (IB) dual-coolant lead–lithium (DCLL) breeding blanket, where eutectic alloy lead–lithium (PbLi) is used as the breeder material and coolant, ferritic steel (FS) as the structural material, helium (He) gas as the coolant for the first wall and the FS structure, and the flow channel insert (FCI) made of silicon carbide (SiC), either composite or foam, as electric and thermal insulator. The R&D for the outboard (OB) blanket for the DEMO concept was initiated earlier, in 2004. The design of the OB blanket is outlined in [1] and the detailed magnetohydrodynamic (MHD) and heat transfer analysis for PbLi flows is presented in [2–4]. The IB blanket modules themselves and associated PbLi flow as well as He flow paths in each IB blanket module are similar to those developed earlier for the OB blanket (for details of the OB blanket see already mentioned Refs. [2–4]) and thus are not explained here in detail. The PbLi flow path in the blanket modules includes the inlet manifold, where the PbLi is distributed into the long poloidal ducts; the poloidal ducts themselves, including upward and downward flows; and the outlet manifold, where the hot PbLi is collected before exiting the module. The design of the inlet and outlet manifolds of the IB blanket and the flow channel inserts are assumed to be similar to those in the OB blanket. Further modifications of the IB blanket design, if necessary, will be added in the future. The characteristic features of the IB design compared to the OB blanket are related to the restricted available space, lower heat load (the average neutron wall load is 1.33 MW/m$^2$), long poloidal path of the PbLi flows, and significantly higher magnetic field: 10–12 T against 4–6 T at the OB region. The strong magnetic field and its associated gradients at the edges of the toroidal field coils (TF coils) are the main factors resulting in higher MHD pressure drops compared to the OB blanket, where the total MHD pressure drop was estimated at ~0.4 MPa, which is significantly lower than the recommended maximum allowable pressure drop (~2 MPa).

In the reference pre-conceptual design, the inboard region is subdivided in the poloidal direction into 6 blanket modules: 3 upper modules above the mid-plane and 3 lower modules below. There are totally 96 inboard modules, carrying a total thermal power of 359 MW. Approximately half of this power is carried by PbLi and half by He. The upper and lower modules and associated access ducts are symmetric with respect to the chamber mid-plane. Fig. 1 sketches the 3 lower modules, showing also one TF coil and access ducts connected to the back of the modules. Each PbLi and He access duct includes one external and one internal co-axial duct. The "hot" PbLi moving out of the module flows through the internal duct, while the "cold" liquid entering the module flows through the gap between the two ducts. Such a countercurrent flow does not require as much space as the alternative design with the separated access ducts presently employed in the ITER TBM, where the flows "in" and "out" are fully decoupled. The "cold" PbLi flowing through the gap also provides cooling of the internal duct. The access ducts go outside the magnet space through the space between the TF coils, experiencing strong magnetic field gradients ("fringing magnetic field"). The access ducts for the modules are of different length depending on the poloidal location of a particular module. The longest access duct is 4.2 m. Each blanket module is 1.4 m high and 1.4 m wide. The radial thickness of the IB blanket is 0.5 m. There are 12 poloidal ducts in each module: 6 front and correspondingly 6 rear ducts of the cross-section 0.2 m × 0.2 m each. The access ducts as well as the PbLi ducts in the blanket module itself have a SiC flow insert, which serves as electric insulator to reduce the MHD pressure drop, and as thermal insulator to decouple hot PbLi from the ferritic structure. The PbLi enters the blanket at the temperature

* Corresponding author. Tel.: +1 310 794 5366.
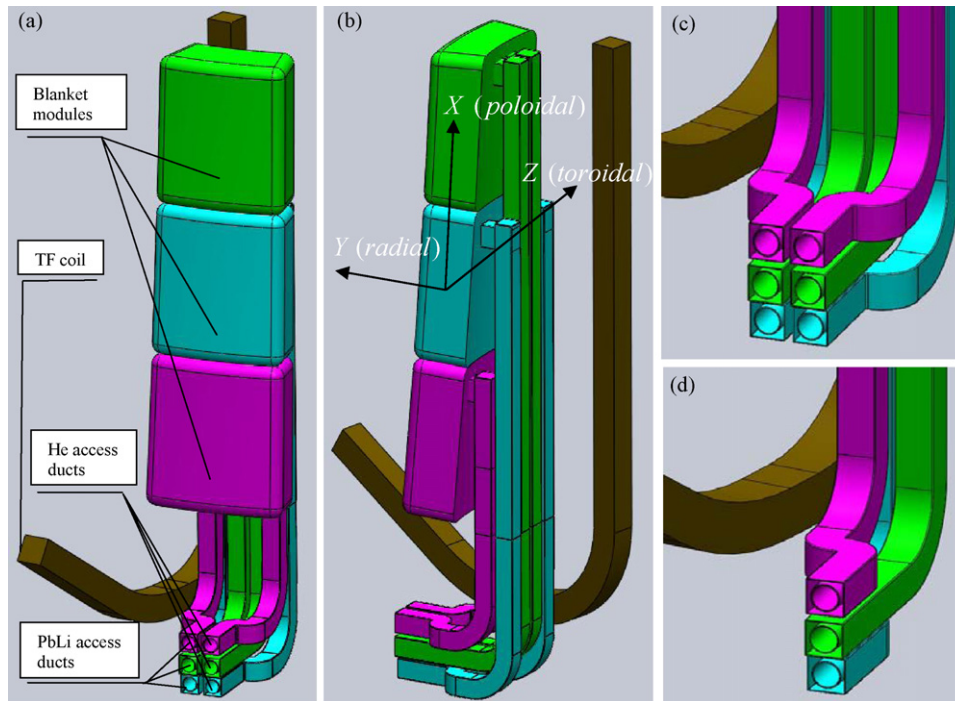E-mail address: sergey@fusion.ucla.edu (S. Smolentsev).

**Fig. 1.** Sketch of the IB region of the DEMO blanket. Only 3 lower blanket modules with access ducts and one TF coil are shown. (a) Front view. (b) Rear view. (c) He and PbLi access ducts. (d) PbLi access ducts only.

$T_{in}$ = 450 °C and leaves at $T_{out}$ = 700 °C. The $\Delta T = T_{out} - T_{in}$ = 250 K is provided via the PbLi bulk velocity in the poloidal flows in the blanket at ∼0.015 m/s (the mass flow rate per module is 35.0 kg/s).

As a variant of this IB blanket design, one can consider a modification, where the breeding modules are attached to a structural ring serving at the same time as a neutron shield and coolant manifold. In such a design, there will be also larger coolant access pipes entering the vacuum vessel between the coils in the radial direction. The flow channel inserts can also be made of a few smaller pieces, about 50 cm each, overlapping at the junctions similar to the roof tiles. These details are however not considered here.

The main components of the PbLi loop that may have the greatest impact on the MHD pressure drop are the following: (A) flows in the poloidal blanket ducts with FCI; (B) flows at the module inlet and outlet; (C) flows in the access ducts in a near-uniform and (D) fringing magnetic field; and (E) flows that change their direction. In addition to calculations of the MHD pressure drops, analysis is performed for the flows in the access ducts. These access duct flows with FCIs have not been analyzed before but such flows can demonstrate increase in the MHD pressure drop and "unusual" flow patterns, *e.g.* due to electric coupling through the common wall. We also analyze the effect of the FCI electric conductivity on the MHD pressure drop in the poloidal flows. In what follows, along with the dimensional parameters, we use dimensionless numbers: the Hartmann number $Ha = B_0 b \sqrt{\sigma/\nu\rho}$ and the interaction parameter $N = (B_0^2 b\sigma/U_m\rho)$, where $B_0$ is the applied (toroidal) magnetic field, $U_m$ is the mean bulk velocity, $b$ is the duct cross-sectional dimension (half of the inner toroidal length of the insert), and $\sigma$, $\nu$ and $\rho$ are the fluid electric conductivity, kinematic viscosity and density, correspondingly.

## 1. Effect of SiC electric conductivity on MHD pressure drop

This analysis is applied to the poloidal flows in the blanket module assuming a 10 T magnetic field. The FCI has a thickness of 5 mm. It is separated from the outer FS duct with a small gap of

2 mm, which is also filled with flowing PbLi. In the present analysis, the electric conductivity of the FCI $\sigma_{FCI}$ is used as a parameter to determine conditions when the FCI acts as ideal insulator. Similar analysis performed for the OB blanket has demonstrated that the near-ideal insulation can be provided with a 5 mm SiC FCI if $\sigma_{FCI}$ < 1 S/m [4]. In the present analysis, the fully developed MHD flow problem is solved numerically for 6 values of $\sigma_{FCI}$. The numerical code solves the MHD equations in a multi-material domain, including the liquid, FS wall and the FCI using a finite-difference technique. For details of the numerical code see Ref. [5].

Fig. 2 shows the effect of the electric conductivity on the dimensionless flow rate defined as $Q = b^{-2} \iint U/[U]dzdy$, where the velocity scale $[U]$ is defined as $[U] = b^2\nu^{-1}\rho^{-1}(-dP/dx)$, and integration is performed over the cross-sectional area inside the FCI
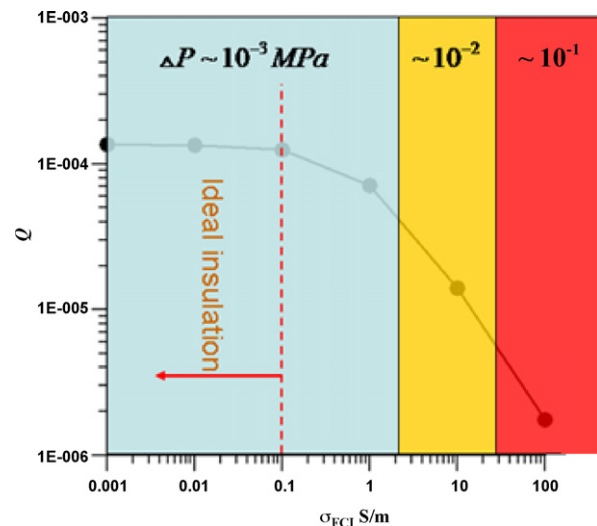


**Fig. 2.** Effectiveness of the 5 mm SiC FCI as electric insulator in the poloidal IB blanket flows in a 10 T magnetic field ($Ha$ = 26,500).
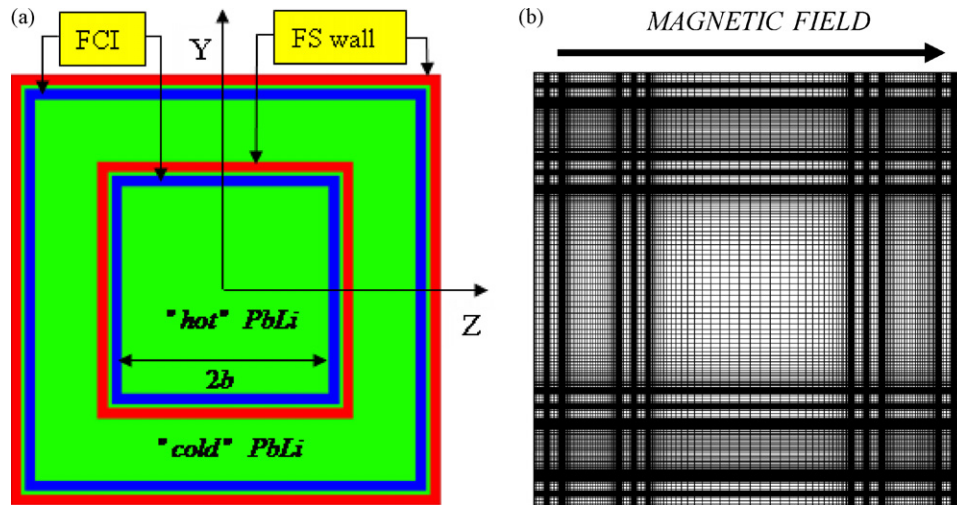
**Fig. 3.** Sketch of the cross-section of the PbLi access duct (a) and the computational mesh (b).

box. The relation between $Q$ and the dimensional pressure gradient is given by $(-dP/dx) = 4U_m \nu \rho b^{-2} Q^{-1}$. The order of magnitude of the MHD pressure drop in the poloidal flow of the reference IB blanket using all the blanket parameters specified above is shown at the top of the figure. When $\sigma_{FCI}$ changes from 0.001 to 100 S/m, the pressure drop ranges in two orders of magnitude (the mean bulk velocity in all cases is the same: $U_m = 0.015$ m/s). It is also seen that the ideal insulation requires $\sigma_{FCI} < 0.1$ S/m. However even at $\sigma_{FCI} = 1$ S/m, $Q$ does not differ much from that in the case of ideal insulation. Therefore, using a 5 mm FCI at $\sigma_{FCI} = 1$ S/m in the IB blanket provides almost maximum effect on the pressure drop reduction. Recent experiments show that $\sigma_{FCI}$ can be maintained at ~10 S/m for 2D SiC composites [6]. Lower values ~1 S/m seem to be achievable, if necessary, using SiC foams as suggested in [7].

## 2. MHD flow in the access ducts

Three geometries of the access duct are among the candidates for the reference design: (i) the internal and external ducts are rectangular; (ii) the external duct is rectangular while the internal one is circular (see Fig. 1); and (iii) both ducts are circular. In all cases the access ducts have two insulating flow inserts: one is inside the internal duct, and the other in the gap between the two ducts. There is no FCI on the outer surface of the internal duct to provide good cooling conditions of the internal FS duct by the "cold" PbLi flowing in the gap. Although the MHD pressure drop in all these cases is of the same order, the flow and its effect on cooling conditions can vary and therefore analysis is required for all geometries. In the present study, we limit our considerations to the case of two coaxial rectangular ducts as shown in Fig. 3. Hereinafter, in all poloidal flows $z$ denotes the toroidal distance, while $x$ and $y$ are the poloidal and radial distances, correspondingly. For the sake of simplicity the access ducts in the analysis are limited to the square shape. As a first approximation, we also neglect smaller radial and poloidal field components as well as the spatial variations of the toroidal field. The latter requires full 3D modeling, which is hardly possible for the inboard region with the existing CFD tools. The magnetic field gradients inside the TF coil region are however much smaller compared to the fringing field gradients at the TF coil edges. Although the detailed structure of the flow in a fringing magnetic field is not analyzed here, the associated MHD pressure drop in the access ducts is estimated in the next paragraph.

The countercurrent flow in the access duct is computed using the already mentioned finite-difference MHD code [5] on the mesh shown in Fig. 3b. The volumetric flow rate in the internal duct and

that in the gap between the two ducts are the same as required by mass conservation, while the pressure drop between the two flows can be different. Thus, the pressure drop in the gap between the two ducts is used as the iteration parameter: it is corrected in the course of the computations until the two flow rates become equal and the whole flow does not change any more. The additional iteration loop required for equalizing the two flow rates results in much longer computations compared to the single duct flow. That is why the numerical computations presented in this paper are limited to only a few cases and the pressure equalization slot in the FCI is not included. The effect of the pressure equalization slot on the flow in a single rectangular duct is discussed in detail in [2]. Similar and even more complicated effects due to closing the electric circuit through the slot are likely to occur in the reference countercurrent flow depending on the slot location and the FCI electric conductivity. In fact, as discussed in [2], in ducts with conducting FCI, pressure equalization occurs due to electric currents crossing the FCI even without the pressure equalization openings, so that openings may not be required. The flow structure computed in this way is illustrated in Fig. 4 for the ideally insulating ($\sigma_{FCI} = 0$) and electrically conducting ($\sigma_{FCI} = 10$ S/m) FCI at the Hartmann number $Ha = 5300$, which corresponds to the magnetic field of 4 T. In the computations, the dimension $b$ of the internal duct is 0.05 m, the FS wall thickness is 0.005 m, the FCI thickness is 0.005 m, the gap between the FCI and the FS wall is 0.002 m, and the gap between the two ducts is 0.03 m wide. For this case, the MHD pressure drop in the gap flow is about two times smaller than that in the internal duct. Similar computations have also been performed for a 10 T magnetic field demonstrating the same features (the reason for showing here results computed at lower magnetic field is that fine flow details in the case of 10 T magnetic field are not very well seen in the figures).

Regardless the values of $\sigma_{FCI}$, the flows in the two sections of the gap perpendicular to the magnetic field are almost stagnant so that all "cold" PbLi flow occurs through the two parallel sections. Moreover, in the case of the electrically conducting FCI, the velocity in the perpendicular sections is slightly positive (see Fig. 4b), i.e. the flow direction is opposite to the main flow direction in the gap. Such a velocity distribution in the gap is not favorable for cooling the FS wall that may result in the wall temperature comparable with the "hot" liquid metal temperature in the internal duct, i.e. around 700 °C. From this point of view, other access duct geometries, e.g. one made of circular pipes, looks more attractive as we expect the flow in the gap to be more uniform, but the problem with the stagnant or even reverse flows at the locations where the magnetic field and the wall are perpendicular still remains. The temperature field
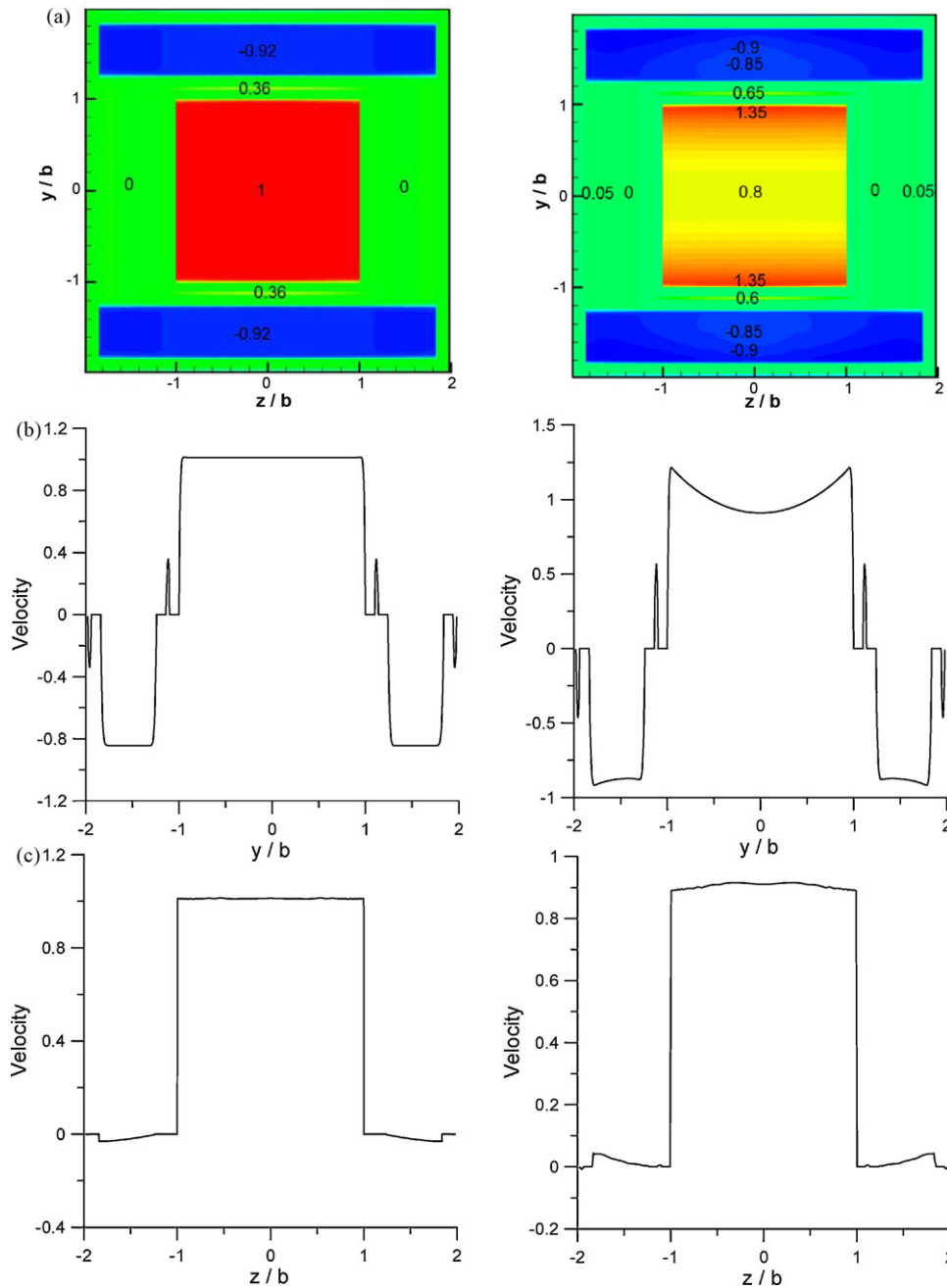
**Fig. 4.** Velocity distribution in the access PbLi poloidal duct: perfectly insulating FCI at $\sigma_{FCI} = 0$ (left) and conducting FCI at $\sigma_{FCI} = 10$ S/m (right). The velocity is scaled with the mean bulk velocity in the internal duct. (a) 2D distribution. (b) 1D distribution across the magnetic field at $z = 0$. (c) 1D distribution along the magnetic field at $y = 0$. Results are shown for $Ha = 3500$.

can also be affected by the velocity pulsations due to MHD turbulence and flow instabilities, probably resulting in better cooling conditions. These mechanisms will need to be considered in the future. It should be mentioned that similar countercurrent flows in access ducts made of SiC (but without a flow insert) were studied analytically in [8,9] for the European Tauro blanket concept, where some increase in the MHD pressure drop due to electric coupling and flow patterns unfavorable for heat transfer, especially if the common wall is electrically conducting, were first observed.

## 3. Total MHD pressure drop

The MHD pressure drop in the whole PbLi loop includes the 3D part $\Delta P_{3D}$ and the part associated with the nearly fully developed

flows in poloidal ducts. MHD pressure drops in the poloidal flows, *i.e.* those in the blanket itself and in the access ducts, were computed numerically for the 10 T magnetic field, $\sigma_{SiC} = 1$ S/m, and the duct dimensions specified above. In these flows, the MHD pressure drop is of order of $10^{-3}$ MPa, which is negligibly small compared to the 3D MHD pressure drops. The 3D MHD pressure drops for the design sketched in Fig. 1 are those due to the flows in the inlet and outlet manifolds in the blanket itself, and in the access ducts associated with the strong magnetic field gradients. The 3D MHD pressure drops associated with geometrical changes are computed with a widely used approach (see *e.g.* [10]) based on the empirical correlation $\Delta P_{3D} = \xi(0.5)\rho U_m^2$, where $\xi$ is the local pressure drop coefficient. The MHD pressure drops due to changes in the flow direction are small as all these changes occur in the planes perpen-

**Table 1**
3D MHD pressure drop in the IB blanket and access ducts.

| 3D flow | Ha | N | k | $\Delta P_{3D}$ (MPa) |
|---|---|---|---|---|
| Blanket inlet manifold | 26,500 | 7000 | 1.5 | 0.49 |
| Blanket outlet manifold | 26,500 | 7000 | 1.5 | 0.49 |
| Access duct (internal) fringing field | 13,250 | 930 | 0.2 | 0.13 |
| Access duct (annulus) fringing field | 26,500 | 3750 | 0.2 | 0.06 |

dicular to the magnetic field. The experimental data suggest $\xi = kN$, where $k$ is the empirical coefficient that depends strongly on the flow geometry. Typically, for flows with geometrical changes in a uniform magnetic field $0.25 < k < 2$ [10–13]. In the calculations, we use higher $k$ for the flows in the inlet/outlet manifolds due to their complexity since the flow is distributed from the radial access duct into parallel poloidal flows or vice versa (for details of the manifold design see [14]). The same empirical correlation is used in the computations of the MHD pressure drop for flows in a fringing magnetic field for which Ref. [15] recommends $k = 0.2$. The results for the 3D MHD pressure drops are summarized in Table 1, showing the total MHD pressure drop in the IB blanket, including the access ducts, 1.17 MPa.

## 4. Concluding remarks

The present analysis shows that the MHD pressure drop in the IB DCLL blanket under DEMO conditions is ~1.17 MPa. Most of the pressure drop originates from the 3D flows in the blanket inlet/outlet manifolds and those in the access ducts due to the strong magnetic field gradients. However, the correlations used in the calculations of the 3D MHD pressure drop are based on the empirical data and include our subjective choice of the coefficient $k$. Therefore, the calculated MHD pressure drop is correct by the order of magnitude, but more accurate assessments will be needed in the future, so that the current numbers can be changed even to lower values. Any modifications of the reference design, including the ring manifold discussed above and overlapping FCIs, will likely lead to a higher MHD pressure drop, possibly approaching closely to the 2 MPa limit.

Our analysis of the effect of $\sigma_{FCI}$ shows that a 5 mm insert provides ideal insulation if $\sigma_{FCI} < 0.1$ S/m. In practice, higher electric conductivities are still tolerable. For $\sigma_{FCI} \sim 1$ S/m, the MHD pressure drop in the fully developed poloidal flows is ~$10^{-3}$ MPa. It becomes ~$10^{-2}$ and ~$10^{-1}$ MPa if $\sigma_{FCI} \sim 10$ and ~100 S/m, correspondingly (see Fig. 2). Thus, the electric conductivity should not be higher than ~10 S/m (for the 5 mm FCI).

The computations of the MHD flow in the access ducts have shown that there can be stagnant or recirculating flow zones inside the gap between the two ducts. Such flows can demonstrate a lack of cooling. Other access duct geometries and possible turbulence effects should be accessed in the future to address cooling condi-

tions in the areas where the magnetic field is perpendicular to the duct wall. The access duct geometry of two concentric circular ducts seems to be a better option compared to two rectangular ducts presently considered because of a more uniform flow distribution, although this design will also experience some flow reduction and possibly recirculation flows in the "Hartmann-part" of the gap [9].

## References

[1] C.P.C. Wong, S. Malang, M. Sawan, S. Smolentsev, S. Majumdar, B. Merrill, et al., Assessment of first wall and blanket options with the use of liquid breeder, Fusion Sci. Technol. 47 (2005) 502–509.
[2] S. Smolentsev, N.B. Morley, M. Abdou, MHD and thermal issues of the SiC$_f$/SiC flow channel insert, Fusion Sci. Technol. 50 (2006) 107–119.
[3] S. Smolentsev, M. Abdou, N.B. Morley, M. Sawan, S. Malang, C. Wong, Numerical analysis of MHD flow and heat transfer in a poloidal channel of the DCLL blanket with a SiC$_f$/SiC flow channel insert, Fusion Eng. Des. 81 (2006) 549–553.
[4] S. Smolentsev, N.B. Morley, C. Wong, M. Abdou, MHD and heat transfer considerations for the US DCLL blanket for DEMO and ITER TBM, Fusion Eng. Des. 83 (2008) 1788–1791.
[5] S. Smolentsev, N. Morley, M. Abdou, Code development for analysis of MHD pressure drop reduction in a liquid metal blanket using insulation technique based on a fully developed flow model, Fusion Eng. Des. 73 (2005) 83–93.
[6] Y. Katoh, L. Snead, Operating temperature window for SiC ceramics and composites for fusion energy applications, Fusion Sci. Technol. 56 (2009) 1045–1052.
[7] S. Sharafat, A. Aoyama, N. Morley, S. Smolentsev, Y. Katoh, B. Williams, et al., Development status of a SiC-foam based flow channel insert for a US-ITER DCLL TBM, Fusion Sci. Technol. 56 (2009) 883–891.
[8] L. Bühler, Poloidal MHD flow in the European TAURO blanket concept, Technical Report FZKA 6384, Forschungszentrum Karlsruhe GmbH, 1999.
[9] L. Bühler, Magnetohydrodynamic flow in the European Tauro blanket concept, Fusion Eng. Des. 61–62 (2002) 471–476.
[10] P. Norajitra, L. Bühler, A. Buenaventura, E. Diegele, U. Fisher, S. Gordeev, et al., Conceptual Design of the Dual-Coolant Blanket within the Framework of the EU Power Plant Conceptual Study (TW2-TPR-PPCS12). Final Report FZKA 6780. Forschungszentrum Karlsruhe GmbH, 2003.
[11] V.N. Demyanenko, B.G. Karasev, A.F. Kolesnichenko, I.V. Lavrent.ev, O.A. Lielausis, E.V. Muravev, et al., Liquid metal in the magnetic field of a TOKAMAK reactor, Magnetohydrodynamics 24 (1988) 95–114.
[12] G.K. Grinberg, M.Z. Kaudze, O.A. Lielausis, Local MHD resistance on a liquid sodium circuit with a superconducting magnet, Magnetohydrodynamics 21 (1985) 99–103.
[13] A.V. Tananaev, T.N. Aitov, A.V. Chudov, V.A. Shmatenko, Linear approximation application limits in MHD-flow theory for strong magnetic fields. Experimental results, in: J. Lielpetris, R. Moreau (Eds.), Liquid Metal Magnetohydrodynamics, Kluwer, 1989, pp. 37–43.
[14] K. Messadek, M. Abdou, Experimental study of the MHD flow in a prototypic inlet manifold section of the DCLL blanket, Magnetohydrodynamics 45 (2009) 233–238.
[15] O. Lielausis, Liquid–metal magnetohydrodynamics, Atomic Energy Review 13 (1975) 527–581.